NOTES AND CORRESPONDENCE

The Effect of Enhanced Greenhouse Warming on Winter Cyclone Frequencies and Strengths

STEVEN J. LAMBERT

Canadian Centre for Climate Modelling and Analysis, Victoria, British Columbia, Canada

11 June 1993 and 27 October 1994

ABSTRACT

The extratropical winter cyclone climatologies for the Northern and Southern Hemispheres are presented for a control, or $1 \times CO_2$ simulation, and an enhanced greenhouse warming, or $2 \times CO_2$ simulation, using the second generation Canadian Climate Centre general circulation model. When compared to the control climatology, the $2 \times CO_2$ simulation exhibits a significant reduction in the total number of lows in both winter hemispheres. Although the total number of cyclones decreases, the frequency of intense cyclones increases, with this behavior being more significant in the Northern Hemisphere. Examination of the storm tracks in both simulations indicates that there is little change in their geographical positions with global warming.

1. Introduction

Cyclones play an important role in the observed climate. Areas influenced by migratory cyclones experience frequent cloudiness and precipitation. These areas also experience a relatively high variability caused by the alternation between cyclonic and anticyclonic regimes. It is argued in the IPCC (1990) report and elsewhere that changes in variability and especially extreme events are as or more important than changes in means.

The increase in the concentration of radiatively active gasses in the atmosphere enhances the greenhouse effect. Modeling studies suggest that this will result in a general cooling of the stratosphere and a warming of the troposphere. The tropospheric warming is expected to be greater in polar regions than in the Tropics, greater over continents than over oceans, and greater in winter than in summer. This differential warming should lead to a reduction of the pole to equator temperature gradient in the lower troposphere. This in turn would be expected to lead to reduced baroclinic activity, especially during winter, and as a result, the number of extratropical cyclones might be expected to decrease.

The question of the influence of global warming on midlatitude cyclone frequencies may be addressed by the use of general circulation models (GCM). The simulations from these models are able to provide information on changes in geographical distribution, intensity, and frequency of cyclones that might occur in a warmer world.

The present paper gives the changes in the cyclone climatology in a $2 \times CO_2$ equilibrium case as simulated by the Canadian Climate Centre (CCC) second generation GCM (GCMII). The model, which is described in detail in McFarlane et al. (1992), is a 10-level spectral model with a horizontal triangular truncation at 32 waves. The model incorporates a thermodynamic sea ice model and a "slab" ocean model to which flux correction has been applied. Details of the enhanced greenhouse effect equilibrium simulation (the CO_2 was doubled and held constant during the simulation) performed with this model are described in Boer et al. (1992). The global surface temperature change simulated by the model with a doubling of CO_2 is 3.5°C, which is within the IPCC (1990) expected range of 1.5°–4.5°C.

2. Data and analysis

The general procedure used to extract cyclone climatologies is to divide the study region into subareas or "analysis boxes" and enumerate the number of lows that influence each subarea. Typically, the analysis boxes are grid squares or latitude–longitude quadrangles. For the present study, the analysis was done in the following manner. The 1000-mb geopotential was extracted once per day from the last 5 yr of 10-yr simulations of the base, or $1 \times CO_2$, climate and the enhanced greenhouse warming, or $2 \times CO_2$ climate. The geopotential was available as values on a global Gaussian grid with 96 longitudes and 48 latitudes. Next, the

Corresponding author address: Dr. Steven J. Lambert, Canadian Centre for Climate Modelling and Analysis, P.O. Box 1700, MS 3339, Victoria, BC, Canada, V8W 2Y2.
E-mail:acrnrsl@uvic.bc.doe.ca

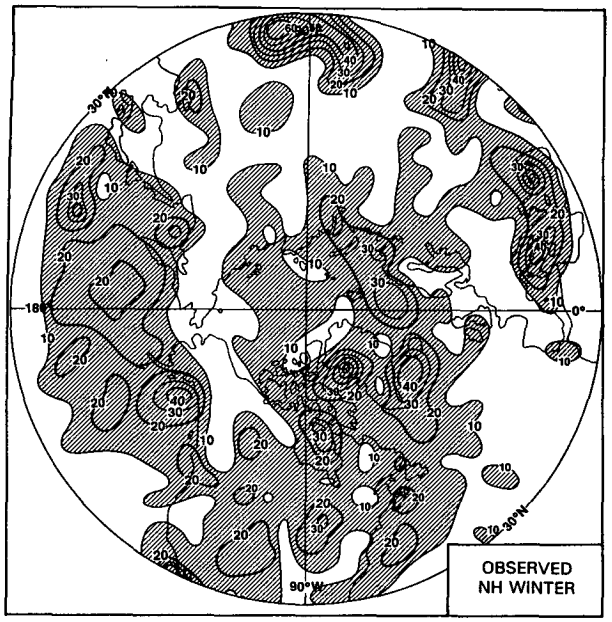

FIG. 1. The total number of cyclone events per 200 000 km^2 for five Northern Hemisphere winters based on ECMWF operational analyses. The contour interval is 10 with values over 10 shaded.

data were transformed to arrays of spherical-harmonic coefficients with a triangular truncation at 32 waves. These coefficients were subsequently synthesized on hemispheric polar stereographic grids with a spacing of about 440 km at 60° lat giving the analysis boxes an area of about 200 000 km^2.

The cyclone frequencies poleward of 30 deg were determined by summing the total number of cyclone events at each grid point, where an event is the occurrence of a value of the geopotential at a grid point that is lower than each of the four surrounding points. A quasi-stationary or slowly moving cyclone will be enumerated many times and it is possible for rapidly moving cyclones to traverse an analysis box without being enumerated at all. The frequencies were computed for five winter seasons (December–February for the Northern Hemisphere and June–August for the Southern Hemisphere).

Using the above procedure, Lambert (1988) (henceforth L88) extracted the cyclone climatology of the first generation CCC GCM (GCMI) (Boer et al. 1984). and an observed climatology based on 5 yr of European Centre for Medium-Range Weather Forecasts (ECMWF) operational analyses. This observed climatology is displayed in Fig. 1. The L88 study showed that features of the cyclone climatology that were thermal in nature, such as east coast storm tracks, were satisfactorily simulated and those that were orographic in nature were poorly simulated. It was also noted that simulated cyclones occluded more slowly than observed ones. Overall, the model produced a reasonably successful qualitative simulation.

TABLE 1. The intensity categories and their range of central heights.

Category	Central height (Z) range
1	$Z > 200$ m
2	200 m $> Z >$ 100 m
3	100 m $> Z >$ 0 m
4	0 m $> Z > -100$ m
5	-100 m $> Z > -200$ m
6	-200 m $> Z > -300$ m
7	-300 m $> Z > -400$ m
8	-400 m $> Z > -500$ m
9	-500 m $> Z$

Some of the following results are presented as a function of cyclone intensity by enumerating the cyclone events in each of nine intensity categories based on the 1000-mb height at the low center. The intensity categories are given in Table 1. Table 2, taken largely from L88, displays the number of observed cyclone events based on ECMWF operational analyses, the number of events simulated by GCMI, and the number of events from the base climate of GCMII for five Northern and Southern Hemisphere winters. From these results, it is evident that GCMI exhibited fewer events than observed. For the Northern Hemisphere, the fraction is about 75% and about 90% for the Southern Hemisphere. The results for the new version of the model (GCMII) will be discussed in subsequent sections.

3. Results

The number of cyclone events per 200 000 km^2 for five winter seasons in the Northern Hemisphere from the 1 × CO_2 simulation of GCMII is displayed in Fig. 2. Since there were 450 samples taken during the five winter seasons, the percentage of the time that a grid

TABLE 2. Number of cyclone events over five winters as a function of central pressure from observations (Obs), GCMI, and GCMII. The observation-based results are from ECMWF/WMO analyses.

	Cyclone events					
	Northern Hemisphere			Southern Hemisphere		
Category	Obs	GCMI	GCMII	Obs	GCMI	GCMII
1	201	50	542	9	1	31
2	1654	653	1952	358	264	681
3	2510	1676	2509	772	938	1086
4	1733	1354	2520	1099	1178	2166
5	1034	1102	1357	1785	1534	2831
6	365	530	500	1538	1151	1711
7	64	181	123	541	439	438
8	15	30	11	52	67	47
9	2	2	0	8	9	0
Total	7578	5578	9596	6162	5581	8991

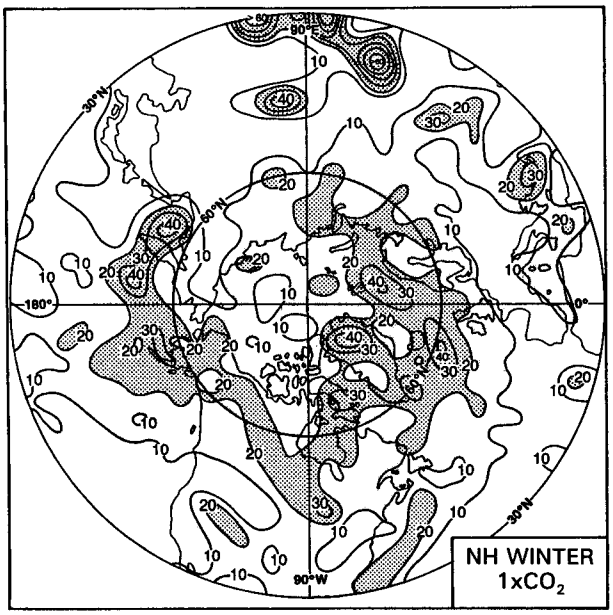

FIG. 2. The total number of cyclones events per 200 000 km^2 for five Northern Hemisphere winters from the 1 × CO_2 or control simulation of the CCC GCMII. The contour interval is 10 and values over 20 are shaded.

square experienced a cyclone event can be obtained by dividing the number of events by 4.5. Figure 2 can be compared to the standard climatologies of Petterssen (1956), Klein (1957), and Figure 1. In the Pacific Ocean there are two principal tracks present in the observations. One begins near 30°N, south of Japan, and extends to the Gulf of Alaska. The other originates in the Sea of Okhotsk and also extends to the Gulf of Alaska. The more southern of these is observed to exhibit the higher cyclone frequencies. Both of these tracks are present in the model simulations. However, the southern track, exhibiting about 70% of the cyclone frequencies given in Petterssen (1956), is somewhat weaker and the northern track considerably stronger than observed. In addition, the two model storm tracks do not terminate abruptly in the Gulf of Alaska as observed but continue into northern Canada. The observations indicate high cyclone frequencies in the lee of the Rockies that are not well reproduced by the model. This behavior suggests a problem in the treatment of topography in the model that might improve with increased resolution. In spite of weak lee cyclogenesis, the cyclone frequency maxima near the Great Lakes and Hudson bay are well simulated. In the Atlantic Ocean, the observations show a storm track that originates off the southeastern coast of the United States and extends northeastward. The track splits south of Greenland with one branch terminating in northern Europe and the other in Davis Strait. The model captures this storm track rather well except that the Davis Strait branch is found over the high terrain of Greenland. The observations indicate an area of very high cyclone frequencies in the Mediterranean with maxima in the Gulf of Genoa and south of Turkey. Both maxima are present in the model simulations, but weaker than observed; especially that in the Gulf of Genoa.

The results of Fig. 2 indicate that, in general, the model produces a reasonable simulation of the Northern Hemisphere winter cyclone frequencies. It is more successful than GCMI in the Mediterranean, where the more recent model captures some of the Genoa cyclone activity. Comparison of the 1 × CO_2 results of GCMII with the observed values given in L88 shows that the new model's total cyclone frequencies are about 25% higher than observed, whereas, as mentioned previously, GCMI simulated too few cyclone events. The additional cyclone events found in GCMII compared to GCMI tend to be randomly distributed over the hemisphere and do not exhibit a tendency to occur in specific geographical areas. The reason for this difference between the two models is not clear. Since they differ in many respects, such as resolution, physical parameterizations, and the inclusion of ocean and sea-ice models, additional sensitivity experiments would be needed to determine the effect of each on the simulated cyclone events.

Figure 3 gives the Northern Hemisphere cyclone frequencies for the enhanced greenhouse warming simulation. Comparison of these results to Fig. 2 shows that the geographical positions of the storm tracks are essentially unchanged. There is an overall reduction of cyclone frequencies as indicated by a "thinning" of the storm tracks. However, in areas where the storm tracks originate, for example, off the southeastern United

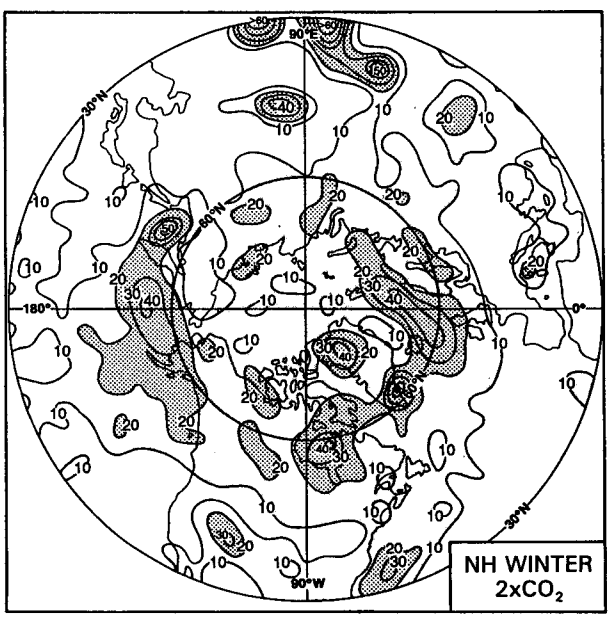

FIG. 3. Same as Fig. 2 except for the 2 × CO_2 or enhanced greenhouse house warming simulation.

States and over the Sea of Okhotsk, the 2 × CO_2 simulation shows higher frequencies.

Figure 4 displays the fraction of the total number of cyclone events for the Northern Hemisphere in each of the intensity categories listed in Table 1. The fraction was computed by dividing the number of events in each category by the total number of simulated or observed events summed over the nine categories. Results are given for the real atmosphere based on ECMWF operational analyses, GCMI taken from L88, and the 1 × CO_2 simulation of GCMII. The observed results exhibit a maximum in category 3. GCMI also displays a maximum in category 3, but the fractions are too large in categories 4 to 9 and too small in category 2. GCMII has a broad peak in categories 3 to 4. In general, GCMII tends to follow the observations more closely than GCMI indicating further the improvement realized with the second generation model.

Table 3 displays the total number of cyclone events and the number of cyclone events as a function of central height for the Northern Hemisphere winter. Results are given for the 1 × CO_2 simulation, the 2 × CO_2 simulation, and the differences (2 × CO_2 values minus 1 × CO_2 values) between them and the Students t value for the differences. The t statistic is computed using

$$t = \frac{\bar{x}_2 - \bar{x}_1}{\left\{\left(\frac{1}{n_2} + \frac{1}{n_1}\right)[(n_2 - 1)s_2^2 + (n_1 - 1)s_1^2]\right\}^{1/2}},$$

where $\bar{x}$ is a five-season mean, s is the standard deviation of the seasonal values, and n is the number of seasons. The subscript 1 refers to the control simulation and the subscript 2 refers to the enhanced warming simulation. For the five winter seasons considered here, there are eight degrees of freedom. For a two-tailed test at the five percent level, t values greater than or equal to 2.3 indicate significant differences between the simulations.

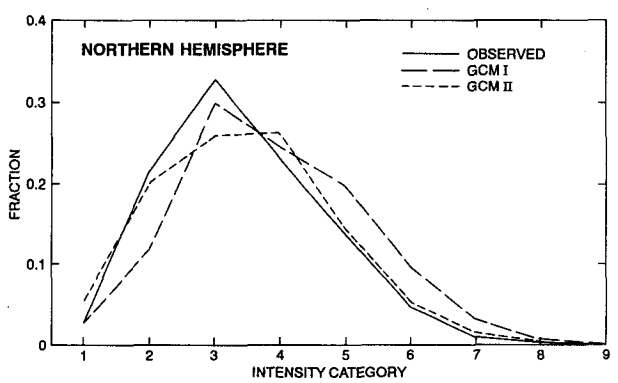

FIG. 4. The fraction of the total number of cyclone events for the Northern Hemisphere found in each of the intensity categories listed in Table 1. The observed results are given by a solid line, the results for GCMI by a long dashed line, and those for GCM II by a short dashed line.

TABLE 3. Number of cyclone events as a function of central height for the Northern Hemisphere north of 30°N for five winters. Included are events from the 1 × CO_2 simulation, the 2 × CO_2 simulation, the differences between them, and the t value for the difference. Values over 2.3 are significant at the five percent level.

	Northern Hemisphere			
Category	1 × CO_2	2 × CO_2	Difference	t value
1	542	373	−151	4.9
2	1952	1815	−137	1.2
3	2509	2122	−387	4.0
4	2520	2425	−95	0.8
5	1357	1560	203	2.4
6	500	596	96	2.4
7	123	154	31	1.6
8	11	23	12	1.0
9	0	1	1	1.0
Total	9596	9069	−427	3.1

The difference for the total events shows a reduction of about four percent for the 2 × CO_2 climate. This difference is significant at the five percent level. The differences as a function of central height show reduced frequency of weak lows and an increased frequency of intense cyclones. The differences are also significant in two categories where increases in cyclone frequencies occur. The reduction of the total number of cyclones accompanied by an increase in intense cyclones is an unexpected result in view of the reduced poleward heat transport required in a warmer world. The increase in the number of more intense cyclones occurs near the terminations of the storm tracks where more mature cyclones are typically observed. A possible contributor to the increased frequency of intense lows is the higher levels of humidity present with global warming. The increased latent heat release could contribute to the development of some cyclones.

The 1 × CO_2 results for the Southern Hemisphere winter are given in Fig. 5. The character of the Southern Hemisphere climatology is markedly different from that of the Northern Hemisphere. The Southern Hemisphere cyclone frequencies are dominated by a circumpolar maximum surrounding Antarctica. Frequencies over Antarctica are higher than observed, which is a further indication that there are problems in simulating the orographic aspects of the cyclone climatology. The fact that cyclones are able to move into Antarctica results in lower than observed frequencies in the circumpolar ring. There is evidence of a midlatitude storm track that originates in the Tasman Sea and merges with the circumpolar ring near South America. The simulated climatology is similar to that of GCMI and agrees well with the results of Taljaard (1967) and the ECMWF-based climatology of L88 displayed in Fig. 6.

Figure 7 displays the distribution of cyclone events in the Southern Hemisphere for the enhanced warming simulation. As was the case for the Northern Hemi-

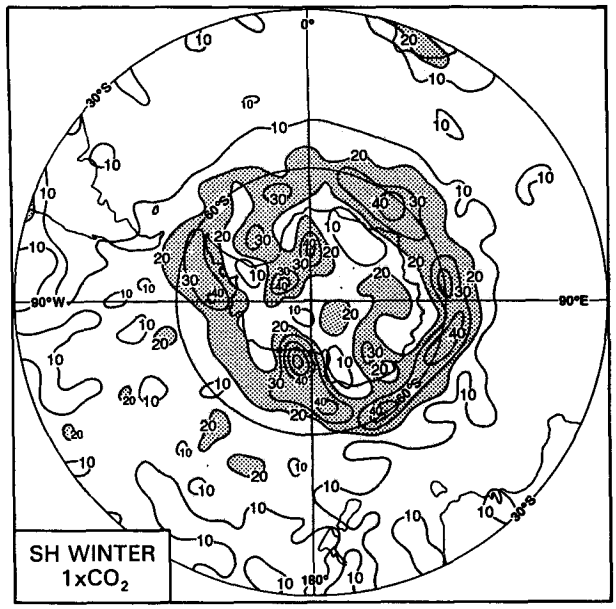

FIG. 5. Same as Fig. 2 except for the Southern Hemisphere.

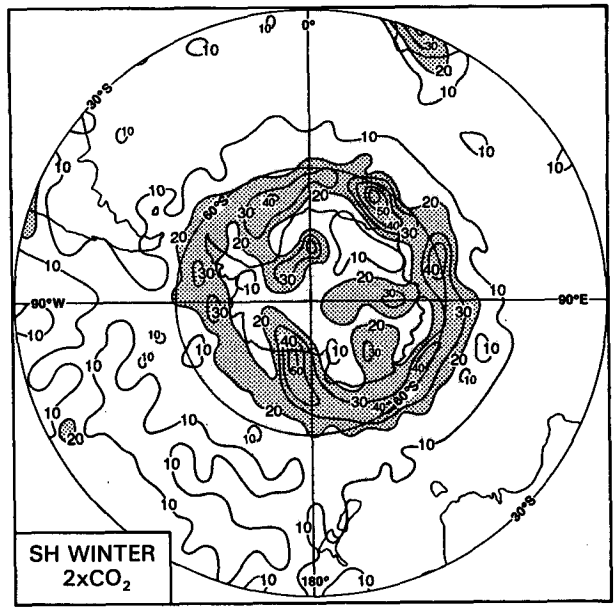

FIG. 7. Same as Fig. 3 except for the Southern Hemisphere.

sphere, there is no obvious latitudinal shift in the storm tracks and there is a general reduction in the number of events.

Figure 8 displays the fraction of observed and simulated events in each intensity category for the Southern Hemisphere. Comparison of these results to those given in Fig. 4 shows that there is a noticeable difference in the behavior of the two hemispheres. It is encouraging to note that both models have been successful in simulating the qualitative aspects of the difference. As was the case for the Northern Hemisphere, the new model simulates more cyclone events than the old model. GCMII produces about 145% of the observed number while GCMI simulates about 90%.

The number of Southern Hemisphere winter events as a function of central height for both the $1 \times CO_2$ and the $2 \times CO_2$ runs as well as the differences between them are given in Table 4. Compared to the control simulation, the $2 \times CO_2$ simulation exhibits a statistically significant five percent reduction in the total number of cyclone events. As was the case for the Northern Hemisphere, the number of intense cyclones increases but is less dramatic than the northern results and generally is not significant.

With the model predictions available, it is useful to examine the observational record for evidence to sup-

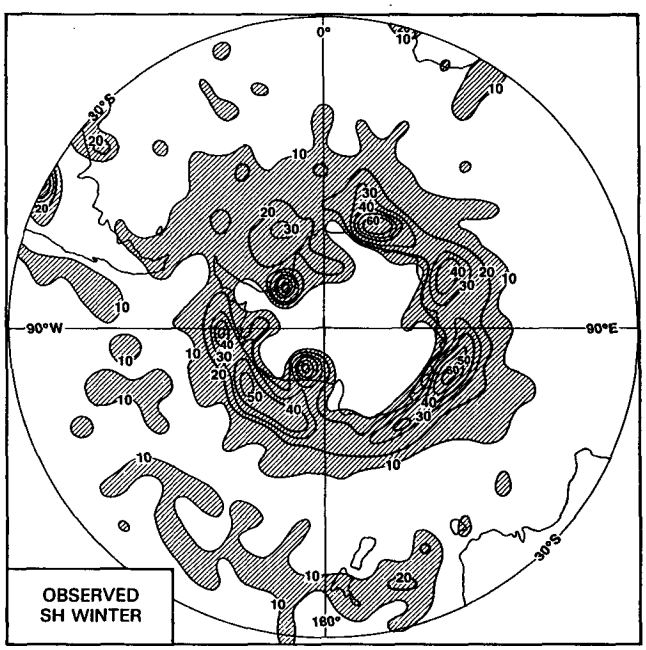

FIG. 6. Same as Fig. 1 except for the Southern Hemisphere.

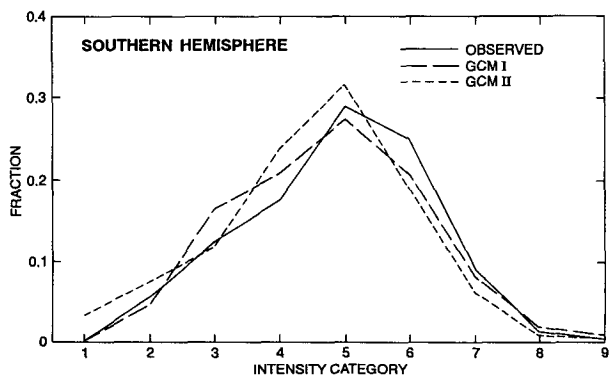

FIG. 8. Same as Fig. 4 except for the Southern Hemisphere.

TABLE 4. Same as Table 2 except for the Southern Hemisphere south of 30°S.

	Southern Hemisphere			
Category	$1 \times CO_2$	$2 \times CO_2$	Difference	t value
1	31	38	7	0.7
2	681	646	−35	0.3
3	1086	1092	6	0.0
4	2166	1788	−378	1.3
5	2831	2689	−142	1.3
6	1711	1745	34	0.2
7	438	461	23	0.3
8	47	67	20	1.1
9	0	5	5	3.1
Total	8991	8531	−460	4.8

port them. A study by Gloersen and Campbell (1991) provides some evidence to support the model predictions of warming in the polar regions. Using satellite data, they observed a significant decrease in Arctic sea-ice cover over the period 1978–1987. There do not appear to be any studies that have examined cyclone frequency trends over the entire extratropics of either hemisphere. The most applicable study is that of Zishka and Smith (1980), which examined cyclone trends over about one-third of the extratropical Northern Hemisphere for the period 1950–1977. Their results are qualitatively consistent with the model simulations in that during the 28-year period, they observed a reduction in the total number of cyclones and an increase in intensity. Although this consistency is interesting, it must be remembered that the Zishka and Smith study did not consider the entire hemisphere and in addition their trends do not agree quantitatively with the model. At best, only a small portion of the trends reported by Zishka and Smith could result from increased warming when one considers that during the 28-year period a warming of only about 0.1°C was observed in the Northern Hemisphere.

4. Summary and conclusions

The extratropical winter cyclone climatologies have been extracted from $1 \times CO_2$ and $2 \times CO_2$ equilibrium simulations by the second generation CCC GCM. The results indicate that global warming may bring a reduction in the total number of lows in both hemispheres. Stratification of the results by cyclone intensity shows an increase in intense lows with this being more evident in the Northern Hemisphere than the Southern Hemisphere. The simulated storm tracks are associated with land–sea temperature contrasts and consequently their positions are relatively insensitive to the enhanced greenhouse effect. Lee cyclogenesis and the resulting storm tracks are not well simulated by the model, and it is likely that the model results are not able to provide useful information on how these features might shift in the real atmosphere with enhanced warming.

REFERENCES

Boer, G. J., N. A. McFarlane, R. Laprise, J. D. Henderson, and J.-P. Blanchet, 1984: The Canadian Climate Centre atmospheric general circulation model. *Atmos.-Ocean,* **22,** 397–429.

——, ——, and M. Lazare, 1992: Greenhouse gas-induced climate change simulated with the CCC second generation general circulation model. *J. Climate,* **5,** 1045–1077.

Gloersen, P., and W. J. Campbell, 1991: Recent variations in Arctic and Antarctic sea-ice covers. *Nature,* **352,** 33–36.

IPCC, 1990: *Climate Change: The IPCC Scientific Assessment.* J. T. Houghton, G. J. Jenkins, and J. J. Ephraums, Eds., Cambridge University Press, 365 pp.

Klein, W. H., 1957: Principal tracks and mean frequencies of cyclones and anticyclones in the Northern Hemisphere. Res. Paper No. 40, U.S. Weather Bureau, U.S. Govt. Printing Office, Washington, DC, 60 pp.

Lambert, S. J., 1988: A cyclone climatology of the Canadian Climate Centre General Circulation Model. *J. Climate,* **1,** 109–115.

McFarlane, N. A., G. J. Boer, J.-P. Blanchet, and M. Lazare, 1992: The Canadian Climate Centre second generation general circulation model and its equilibrium climate. *J. Climate,* **5,** 1013–1044.

Petterssen, S., 1956: *Weather Analysis and Forecasting.* Vol. 1. McGraw-Hill, 422 pp.

Taljaard, J. J., 1967: Development, distribution and movement of cyclones and anticyclones in the Southern Hemisphere during the IGY. *J. Appl. Meteor.,* **6,** 973–987.

Zishka, K. M., and P. J. Smith, 1980: The climatology of cyclones and anticyclones over North America and surrounding ocean environs for January and July, 1950–1977. *Mon. Wea. Rev.,* **108,** 387–401.